JACS
JOURNAL OF THE AMERICAN CHEMICAL SOCIETY

Communication

pubs.acs.org/JACS

Control of Protein-Binding Kinetics on Synthetic Polymer Nanoparticles by Tuning Flexibility and Inducing Conformation Changes of Polymer Chains

Yu Hoshino,* Masahiko Nakamoto, and Yoshiko Miura*

Department of Chemical Engineering, Kyushu University, 744 Motooka, Nishi-ku, Fukuoka 819-0395, Japan

Supporting Information

ABSTRACT: Although a number of procedures to create synthetic polymer nanoparticles (NPs) with an intrinsic affinity to target biomacromolecules have been published, little has been reported on strategies to control the binding kinetics of target recognition. Here, we report an enzyme-mimic strategy to control binding/dissociation rate constants of NPs, which bind proteins through multipoint interactions, by taking advantage of the temperature-responsive coil−globule phase transition of poly-*N*-isopropylacrylamide (PNIPAm)-based NPs. PNIPAm NPs with a "flexible" random-coil conformation had a faster binding rate than NPs with a "rigid" globule conformation; however, the dissociation rate constant remained unchanged, resulting in stronger affinity. The dissociation rate of the "flexible" NPs was decelerated by the "induced-fit"-type conformation change of polymers around the coil−globule phase transition temperature, resulting in the formation of the most stable NP−protein complexes. These results provide a guide for designing plastic antibodies with tailor-made binding kinetics and equilibrium constants.

Synthetic polymer nanoparticles that recognize, capture, and/or release specific biomacromolecules are of significant interest as drug carriers, affinity ligands, and antidotes.[1−3] Recently, nanoparticles (NPs) that recognize target proteins/peptides via multipoint interactions have been achieved by optimizing combinations and populations of functional groups[4−8] and/or imprinting binding-sites[9,10] in poly-*N*-isopropylacrylamide (PNIPAm)-based hydrogel NPs. Some NPs have shown the ability to recognize, neutralize, and/or release target molecules, even in living animals.[10,11] However, the activity of the particles in vivo was significantly lower than that expected based on results from in vitro experiments,[11] since undesired events such as creation of protein coronas on NPs and metabolism of materials compete with the designed function.[12−15] To utilize materials in nonequilibrium living systems, binding kinetics as well as the equilibrium of the target-binding process must be carefully engineered.[11,13,16]

It has been reported that the flexibility[17−19] and conformational changes[20,21] of enzymes play a crucial role on the determination of the binding and dissociation rates of the target binding process. For instance, the target binding/dissociation kinetics of dihydrofolate reductase are determined by motion of a flexible loop that covers the substrate- and coenzyme-binding sites of the protein.[22] Large conformation changes of DNA polymerase accelerate the binding rate and decelerate the dissociation rate of the DNA capture process, resulting in formation of a stable DNA−protein complex.[20,21]

In this study, we mimic the flexibility and conformational change of enzymes to control the binding kinetics of target molecules on synthetic polymer NPs. To induce the flexibility and conformation change of the NPs, we took advantage of the temperature-responsive coil−globule phase transition of PNIPAm-based hydrogel NPs. PNIPAm NPs undergo a coil−globule phase transition at the lowest critical solution temperature (LCST, approximately 37 °C).[23] At 25 °C, PNIPAm chains are in the random-coil conformations, and thus, the PNIPAm NPs are swollen, though they are in the globule conformation and collapsed above their transition temperature as a result of an entropy-driven dissociation of water molecules.[24] ^{1}H NMR revealed that the isopropyl group has a large mobility in the swollen state; however, the mobility decreases substantially upon collapse of the gel.[25] Time-resolved fluorescence anisotropy measurements revealed that a marked reduction in the segmental mobility of the PNIPAm chains also occurs at the onset of the LCST.[26] Therefore, flexibility of PNIPAm chains can be tuned from the "flexible" swollen phase with greater segment and side chain motions to the "rigid" collapse phase depending on temperature. The LCST can be further tuned by incorporating *N*-*tert*-butylacrylamide (TBAm) into NPs.[23]

It has been reported that diffusion of small molecules in the PNIPAm hydrogels can be reversibly switched on and off by collapse and swell phase transition.[27,28] Diffusion rate of the molecules in PNIPAm can be further tuned by hydrophobic interaction.[29,30] Tanaka and co-workers reported that with cationic functional groups, PNIPAm gels capture polyanionic dyes through multipoint interactions.[31] The interaction can be further switched on/off by increasing/decreasing volume density of the functional group with the collapse/swell phase transition of the PNIPAm gels.[31] Shea and co-workers have extended the strategy to protein[3] and peptide[7] targets using functionalized PNIPAm NPs. However, effects of flexibility and conformation changes of PNIPAm NPs on the binding/dissociation rate of the multipoint-protein-binding process have not been revealed. To investigate contribution of the flexibility and conformation change of NPs on the protein-binding

Received: June 21, 2012
Published: September 4, 2012

   dx.doi.org/10.1021/ja306053s | *J. Am. Chem. Soc.* 2012, 134, 15209−15212

process, it is important to maintain the volume density of functional groups, which contact (interact) with target protein, in NPs, because dissociation (equilibrium) constants increase exponentially with the volume density of the functional group in the bulk gels[31] and NPs,[11] then effects of flexibility and conformation changes of NPs would be hidden in the effects of density of functional groups. It is also necessary to compare binding/dissociation rate of NPs with different flexibility at the same temperature, because diffusion constants, which are associated with binding/dissociation constants, increase exponentially with the temperature (the Arrhenius equation). In this study, we carefully prepared NPs having various phase (flexibility) at 25 °C with identical volume-density of functional group and quantified binding/dissociation rate constants on each NPs at the same temperature (25 °C).

As a model of a target molecule that would be recognized by PNIPAm NPs, concanavalin A (Con A), a 104 kDa α-D-mannose-binding protein was selected. It is a homotetrameric protein having 4 mannose-binding sites on the corners of its tetrahedral structure, and each side is 10 nm long.[32] Although the monovalent mannose-Con A interaction is relatively weak (K_d 10^{-3}–10^{-4} M), it can be amplified by multivalency; by clustering a number of mannose units on a polymer chain, a synthetic polymer that recognizes Con A with much stronger affinity can be achieved (K_d 10^{-5}–10^{-8} M).[33] Thus, Con A has been widely used as a model target molecule for the study of synthetic polymer architectures that recognize specific biomacromolecules through multipoint interactions.[34−38]

p-Acrylamidophenyl-α-D-mannopyranoside (**Man**) was synthesized as described (Supporting Information (SI))[36,39] and copolymerized into PNIPAm NPs to prepare NPs that recognize Con A through multipoint interactions (Scheme 1).

Scheme 1. Preparation of ManNPs

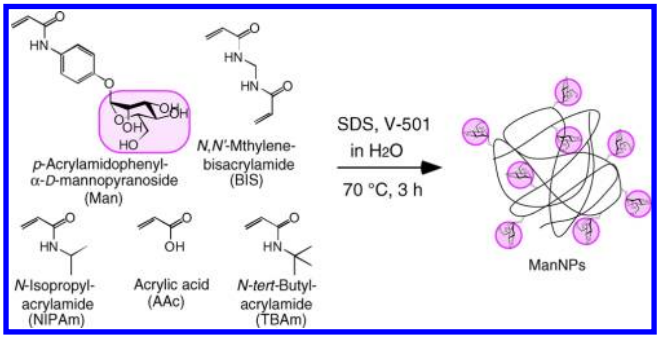

To reveal the influence of flexibility and conformation changes of NPs on the binding kinetics of Con A at 25 °C, NPs with LCST below (**NP1**, <10 °C), above (**NP2**, 37 °C), and around (**NP3**) 25 °C were prepared by tuning the feed ratio of TBAm (Figure 1a). The volume density of **Man** in **NP1**−**NP3** was maintained at 1.0 ± 0.1 molecules/(10 nm)^3 at 25 °C by controlling the feed ratio of **Man**, depending on the swell ratio of each type of NPs (Table S1). It was expected that the **Man** density of 1.0 ± 0.1 molecules/(10 nm)^3 allowed multipoint interactions between several **Man** units on the NPs and a Con A molecule, depending on the flexibility of the polymer chains of the **ManNPs**. Incorporation of **Man** into each NP was quantified by ^{1}H NMR (Figures S1 and S2) and the swell ratios were quantified by dynamic light scattering (DLS). As we designed, **NP1** and **NP2** were in the swollen and collapsed states, respectively, at 25 °C (Figure 1a). Although diameter

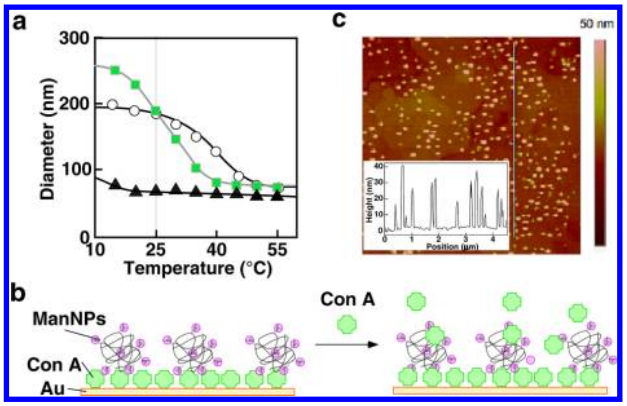

Figure 1. (a) Hydrodynamic diameter of **ManNPs** synthesized with 0% (**NP1**; open circle), 40% (**NP2**; black triangle), and 20% (**NP3**; green square) TBAm as a function of temperature. (b) Schematic of the QCM experiments. **ManNPs** were immobilized on the Au surface of the QCM sensor through Con A-mannose interaction (left). Con A binding on **ManNPs** was monitored on the surface of the sensor following introduction of Con A (right). (c) An AFM image of **ManNPs** (40% TBAm, 2% BIS, 5% AAc, 0.11% **Man**) immobilized on a Au substrate through Con A−mannose interaction. A height profile of the cross section (light blue line) is shown inset.

and swell ratio of **NP3** were almost the same as **NP2** at 25 °C, **NP3** was apparently not in the fully swollen state at 25 °C because **NP3** gradually shrunk around 25 °C (between 20 and 35 °C) (Figure 1a). To represent the state of **NP3** at 25 °C, we defined the state as "transition state". To improve colloidal stability and to control the swell ratios of the NPs, 5 mol % of acrylic acid and 10 mol % of BIS (*N*,*N*′-methylenebisacrylamide) were incorporated into all NPs. All NPs did not form aggregates, and did not show significant size and LCST changes in water for at least one year at room temperature (Figure S3).

The binding rate of Con A to the NPs was monitored and analyzed using a 27 MHz quartz crystal microbalance (QCM) (Figure 1b).[35,40] Prior to studying the binding kinetics, binding specificity between the NPs and Con A was confirmed by several experiments. First, when NPs that had **Man** (**NP1**−**3**) were injected into the QCM cells on which Con A had been immobilized, significant interactions were observed. However, no interaction was observed when the NPs without Man were injected (Figure S4). Second, when Con A was injected into the cells on which only Con A had been immobilized, no interactions were observed (Figure S4); in contrast, when Con A was injected into the cells on which **ManNPs** (**NP1**−**3**) had been immobilized on the surface of Con A, significant interactions were observed (Figure 2a). Furthermore, it was confirmed by atomic force microscopy that immobilization of NPs on the surface of gold (Au (111) on mica, Phasis) was not greater than a single layer (Figure 1c).

Figure 2a shows typical frequency changes as a function of time for the **ManNP**-immobilized QCM in 10 mM phosphate buffer (pH 7.4, 137 mM NaCl, 2.68 mM KCl, 1.8 mM $CaCl_2$, and 0.49 mM $MgCl_2$) responding to the addition of Con A. When Con A was injected into the cell (5−240 nM), the frequency decreased (the mass of Con A on the surface increased) gradually for 10−30 min because of the binding of Con A on the **ManNPs**. Both the binding rate (relaxation time of the binding process) and the binding amount of Con A depended on the concentration of Con A (Figure 2a).

The QCM frequency changes in the Con A binding processes were fit very well by the single exponential function

dx.doi.org/10.1021/ja306053s | J. Am. Chem. Soc. 2012, 134, 15209−15212

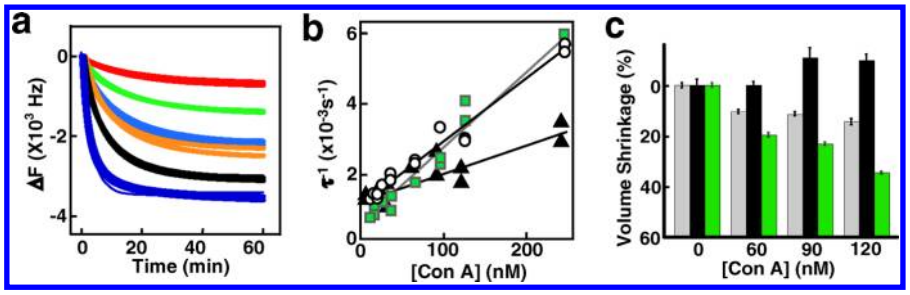

Figure 2. (a) Time courses of frequency changes of **NP1**-immobilized QCM, responding to the addition of 5 (red), 10 (green), 20 (sky blue), 30 (orange), 60 (black), and 240 (blue) nM Con A. Results of duplicated experiments (thick lines) and fit curves (thin lines) are overwritten. (b) Plots of binding relaxation time (τ) on swollen (**NP1**, open circle), collapsed (**NP2**, black triangle), and transition state (**NP3**, green square) NPs as a function of Con A concentration. (c) Volume shrinkage of swollen (**NP1**, gray), collapsed (**NP2**, black), and transition state (**NP3**, green) NPs that were induced by Con A binding.

Table 1. Composition, Phase, Man Density, and Rate/Equilibrium Constants of PNIPAm NPs[a]

NPs	TBAm feed [mol %]	**Man** feed [mol %]	State at 25 °C	Density of **Man** [molecule (10 nm)$^{-3}$]	k_{on} 10^3 $M^{-1}\cdot s^{-1}$	k_{off} 10^{-3} s^{-1}	K_d nM
1	0	1.5	Swollen phase	1.1	18	1.4	78
2	40	0.11	Collapsed phase	0.9	8	1.2	150
3	20	1.5	Transition	0.9	21	0.8	38

[a]10 mol % BIS and 5 mol % AAc were fed in all NPs.

(eq 1, Figure 2a), indicating that the binding event observed in this experiment can be approximated as interaction between Con A and the binding sites on the NPs, each of which has an equal affinity, although the binding site in each of the NPs cannot be homogeneous (SI).[6]

$$\Delta F = \Delta F_{\infty}(1 - e^{-t/\tau}) \quad (1)$$

The reciprocal of the binding relaxation time (τ) for each of the binding processes was plotted against Con A concentration (Figure 2b), showing linear correlations between concentration and τ^{-1} for each type of NPs. These results indicate that the binding process can be approximated as the Langmuir-type binding process given in eq 2 (SI). Apparent binding/dissociation rate constants (k_{on} and k_{off}) for each type of NPs were given as the slopes and y-intercepts of the linear correlations (eq 3, SI):[35,40]

$$\text{ConA} + \text{NP} \rightleftarrows \text{ConA}\cdot\text{NP} \quad (2)$$

$$\tau^{-1} = k_{on}[\text{ConA}] + k_{off} \quad (3)$$

The obtained rate constant k_{on}, k_{off}, and dissociation equilibrium constant K_d ($=k_{off}/k_{on}$) values are summarized in Table 1.

Dissociation constants for **NP1−3** were in the submicromolar range (78, 150, and 38 nM, respectively, Table 1). This number is more than 3 orders of magnitude smaller than the reported monovalent **Man**−Con A interaction (K_d 10^{-3}−10^{-4} M),[33] indicating that Con A binding on **NP1−3** observed in those experiments are all multivalent interactions between more than 2 **Man** units on a particle and one Con A.

Although the dissociation rate constants (k_{off}) of swollen (1.4×10^{-3} s^{-1}) and collapsed (1.2×10^{-3} s^{-1}) NPs were almost equal, the binding rate constant (k_{on}) for the swollen NPs (18×10^3 M^{-1} s^{-1}) was larger than that of the collapsed NPs (8×10^3 M^{-1} s^{-1}). As a result, the dissociation constant (K_d) of the swollen NPs (78 nM) was smaller than that of the collapsed NPs (150 nM). Polymer chains in the swollen gels are in the flexible random-coil conformation with larger segment mobility, whereas the polymer chains are in the rigid globule conformation in the collapsed gels.[24−26] It is suggested that the flexibility of the polymer chains in the swollen NPs allowed mannose to map onto mannose-binding sites on the surface of Con A resulting in faster binding and stabilization of the NP-Con A complexes.

The transition state NPs showed lower dissociation rate constant (0.8×10^{-3} s^{-1}) than the swollen NPs (1.4×10^{-3} s^{-1}), although the binding rate constants of each of the NPs were almost same. Therefore, the transition state NPs showed an even stronger affinity to Con A (K_d = 38 nM) than the swollen NPs (K_d = 78 nM).

To investigate the contribution of conformation changes of polymers on the binding kinetics, volume shrinkage of each of the NPs, which were induced by Con A binding, were estimated by comparing the size of NPs before and after addition of Con A by DLS in 10 mM HEPES buffer (pH 7.4, 1.8 mM $CaCl_2$, and 0.49 mM $MgCl_2$). Interestingly, the volume of the transition state NPs shrunk by 20−40% after addition of a small amount of Con A, depending the on concentration of Con A added (60−120 nM). In contrast, the swollen phase NPs showed a significantly lower degree of size shrinkage (10−15%) than the transition state NPs (Figure 2c). Collapsed NPs did not show any volume shrinkage (Figure 2c). These results indicate that polymer density (steric hindrance) around the binding sites on the transition state NPs after Con A binding was much greater than in the prebinding structure owing to volume shrinkage, resulting in deceleration of the dissociation rate.[41] This is comparable to the "induced-fit" between enzymes or gel catalysts and substrates.[42,43]

From these results, we conclude that binding rates and equilibrium constants can be tuned by the choice of phase of NPs. Swollen phase NPs showed a faster binding rate and stronger affinity than collapsed phase NPs since swollen NPs consist of random-coil-phase polymer chains which are more flexible than the globule-phase chains in collapsed NPs. NPs around the coil−globule phase transition temperature, which is defined as transition state NPs, showed an even stronger affinity than the swollen NPs since bound proteins induced greater conformation change of NPs, resulting in shrinkage of NPs and

dx.doi.org/10.1021/ja306053s | J. Am. Chem. Soc. 2012, 134, 15209−15212

deceleration of dissociation from the NPs. These results provide a general guide that can be used to design "plastic antibodies" with tailor-made binding kinetics and equilibrium constants.

■ ASSOCIATED CONTENT

Supporting Information

Experimental procedures and supporting data. This material is available free of charge via the Internet at http://pubs.acs.org.

■ AUTHOR INFORMATION

Corresponding Author

yhoshino@chem-eng.kyushu-u.ac.jp; miuray@chem-eng.kyushu-u.ac.jp

Notes

The authors declare no competing financial interest.

■ ACKNOWLEDGMENTS

Financial support from MEXT (23111716 and 20106003) and JSPS (23750193) is greatly appreciated.

■ REFERENCES

(1) Nayak, S.; Lyon, L. A. *Angew. Chem., Int. Ed.* **2005**, *44*, 7686.
(2) Hoshino, Y.; Shea, K. J. *J. Mater. Chem.* **2011**, *21*, 3517.
(3) Yoshimatsu, K.; Lesel, B. K.; Yonamine, Y.; Beierle, J. M.; Hoshino, Y.; Shea, K. J. *Angew. Chem., Int. Ed.* **2012**, *51*, 2405.
(4) Hoshino, Y.; Urakami, T.; Kodama, T.; Koide, H.; Oku, N.; Okahata, Y.; Shea, K. J. *Small* **2009**, *5*, 1562.
(5) Cabaleiro-Lago, C.; Quinlan-Pluck, F.; Lynch, I.; Lindman, S.; Minogue, A. M.; Thulin, E.; Walsh, D. M.; Dawson, K. A.; Linse, S. *J. Am. Chem. Soc.* **2008**, *130*, 15437.
(6) Hoshino, Y.; Haberaecker, W. W., III.; Kodama, T.; Zeng, Z.; Okahata, Y.; Shea, K. J. *J. Am. Chem. Soc.* **2010**, *132*, 13648.
(7) Lee, S.-H.; Hoshino, Y.; Randall, A.; Zeng, Z.; Baldi, P.; Doong, R.-A.; Shea, K. J. *J. Am. Chem. Soc.* **2012**, DOI: 10.1021/ja303612d.
(8) Yonamine, Y.; Hoshino, Y.; Shea, K. J. *Biomacromolecules* **2012**, DOI: 10.1021/bm300986j.
(9) Hoshino, Y.; Kodama, T.; Okahata, Y.; Shea, K. J. *J. Am. Chem. Soc.* **2008**, *130*, 15242.
(10) Hoshino, Y.; Koide, H.; Urakami, T.; Kanazawa, H.; Kodama, T.; Oku, N.; Shea, K. J. *J. Am. Chem. Soc.* **2010**, *132*, 6644.
(11) Hoshino, Y.; Koide, H.; Furuya, K.; Haberaecker, W. W.; Lee, S.-H.; Kodama, T.; Kanazawa, H.; Oku, N.; Shea, K. J. *Proc. Natl. Acad. Sci. U.S.A.* **2012**, *109*, 33.
(12) Cedervall, T.; I., L.; Foy, M.; Berggård, T.; Donnelly, S. C.; Cagney, G.; Linse, S.; Dawson, K. A. *Angew. Chem.* **2007**, *119*, 5856.
(13) Cedervall, T.; Lynch, I.; Lindman, S.; Berggård, T.; Thulin, E.; Nilsson, H.; Dawson, K. A.; Linse, S. *Proc. Natl. Acad. Sci. U.S.A.* **2007**, *104*, 2050.
(14) Sun, X.; Rossin, R.; Turner, J. L.; Becker, M. L.; Joralemon, M. J.; Welch, M. J.; Wooley, K. L. *Biomacromolecules* **2005**, *6*, 2541.
(15) Owens, D. E., III.; Peppas, N. A. *Int. J. Pharm.* **2006**, *307*, 93.
(16) Cabaleiro-Lago, C.; Quinlan-Pluck, F.; Lynch, I.; Lindman, S.; Minogue, A. M.; Thulin, E.; Walsh, D. M.; Dawson, K. A.; Linse, S. *J. Am. Chem. Soc.* **2008**, *130*, 15437.
(17) Mittal, S.; Cai, Y.; Nalam, M. N. L.; Bolon, D. N. A.; Schiffer, C. A. *J. Am. Chem. Soc.* **2012**, *134*, 4163.
(18) Kosugi, T.; Hayashi, S. *J. Am. Chem. Soc.* **2012**, *134*, 7045.
(19) Prakash, M. K. *J. Am. Chem. Soc.* **2011**, *133*, 9976.
(20) Dahlberg, M. E.; Benkovic, S. J. *Biochemistry* **1991**, *30*, 4835.
(21) Li, Y.; Korolev, S.; Waksman, G. *EMBO J.* **1998**, *17*, 7514.
(22) Falzone, C. J.; Wright, P. E.; Benkovic, S. J. *Biochemistry* **1994**, *33*, 439.
(23) Debord, J. D.; Lyon, L. A. *Langmuir* **2003**, *19*, 7662.
(24) Nishio, I.; Sun, S.-T.; Swislow, G.; Tanaka, T. *Nature* **1979**, *281*, 208.
(25) Tokuhiro, T.; Amiya, T.; Mamada, A.; Tanaka, T. *Macromolecules* **1991**, *24*, 2936.
(26) Chee, C. K.; Rimmer, S.; Soutar, I.; Swanson, L. *Polymer* **2001**, *42*, 5079.
(27) Bae, Y. H.; Okano, T.; Hsu, R.; Kim, S. W. *Macromol. Chem. Rapid Commun.* **1987**, *8*, 481.
(28) Okano, T.; Bae, Y. H.; Jacobs, H.; Kim, S. W. *J. Controlled Release* **1990**, *11*, 255.
(29) Kim, S. W.; Bae, Y. H.; Okano, T. *Pharm. Res.* **1992**, *9*, 283.
(30) Linse, S.; Dawson, K. A. *J. Phys. Chem. B* **2004**, *108*, 10893.
(31) Oya, T.; Enoki, T.; Grosberg, A. Y.; Masamune, S.; Sakiyama, T.; Takeoka, Y.; Tanaka, K.; Wang, G. Q.; Yilmaz, Y.; Feld, M. S.; Dasari, R.; Tanaka, T. *Science* **1999**, *286*, 1543.
(32) Becker, J. W.; Reeke, G. N.; Cunningham, B. A.; Edelman, G. M. *Nature* **1976**, *259*, 406.
(33) Mann, D. A.; Kanai, M.; Maly, D. J.; Kiessling, L. L. *J. Am. Chem. Soc.* **1998**, *120*, 10575.
(34) Gestwicki, J. E.; Cairo, C. W.; Strong, L. E.; Oetjen, K. A.; Kiessling, L. L. *J. Am. Chem. Soc.* **2002**, *124*, 14922.
(35) Mori, T.; Toyoda, M.; Ohtsuka, T.; Okahata, Y. *Anal. Biochem.* **2009**, *395*, 211.
(36) Toyoshima, M.; Miura, Y. *J. Polym. Sci. A: Polym. Chem.* **2009**, *47*, 1412.
(37) Wang, X.; Ramström, O.; Yan, M. *Adv. Mater.* **2008**, *22*, 1946.
(38) Miyata, T.; Jikihara, A.; Nakamae, K. *Macromol. Chem. Phys.* **1996**, *197*, 1135.
(39) Seto, H.; Ogata, Y.; Murakami, T.; Hoshino, Y.; Miura, Y. *ACS Appl. Mater. Interfaces* **2012**, *4*, 411.
(40) Hoshino, Y.; Kawasaki, T.; Okahata, Y. *Biomacromolecules* **2006**, *7*, 682.
(41) Smith, M. H.; Lyon, L. A. *Macromolecules* **2011**, *44*, 8154.
(42) Wang, G.; Kuroda, K.; Enoki, T.; Grosberg, A.; Masamune, S.; Oya, T.; Takeoka, Y.; Tanaka, T. *Proc. Natl Acad. Sci. U.S.A.* **2000**, *97*, 9861.
(43) Miyata, T.; Jige, M.; Nakaminami, T.; Uragami, T. *Proc. Natl Acad. Sci. U.S.A.* **2006**, *103*, 1190.